NJC

Accepted Manuscript

This is an *Accepted Manuscript*, which has been through the Royal Society of Chemistry peer review process and has been accepted for publication.

Accepted Manuscripts are published online shortly after acceptance, before technical editing, formatting and proof reading. Using this free service, authors can make their results available to the community, in citable form, before we publish the edited article. We will replace this *Accepted Manuscript* with the edited and formatted *Advance Article* as soon as it is available.

You can find more information about *Accepted Manuscripts* in the Information for Authors.

Please note that technical editing may introduce minor changes to the text and/or graphics, which may alter content. The journal's standard Terms & Conditions and the Ethical guidelines still apply. In no event shall the Royal Society of Chemistry be held responsible for any errors or omissions in this *Accepted Manuscript* or any consequences arising from the use of any information it contains.

ROYAL SOCIETY OF CHEMISTRY

www.rsc.org/njc

Journal Name

ARTICLE

A novel preparation of Zr-Si intermetallics by electrochemical reduction of $ZrSiO_4$ in molten salts

Received 00th January 20xx,
Accepted 00th January 20xx

DOI: 10.1039/x0xx00000x

www.rsc.org/

Hongxia Liu [a, b], Yanqing Cai [a], Qian Xu [c,*], Qiushi Song [a], Huijun Liu [d]

A method of controllably preparing Zr-Si intermetallics by the electrochemical reduction of $ZrSiO_4$ and $ZrSiO_4$-SiO_2 mixed powders in molten $CaCl_2$-NaCl at 800 °C is developed. The final product composition can be controlled by adjusting the molar ratio of Si to Zr containing in the starting material, and ZrSi, $ZrSi_2$ and their mixture were obtained by the process. The reduction pathway of $ZrSiO_4$ and SiO_2 to Zr-Si intermetallics undergoes several calcium-containing intermediate phases, such as $CaSiO_3$, Ca_2SiO_4, and calcia-stabilized zirconia (CSZ).

Introduction

Zr-Si intermetallics can be used to produce new structural materials serviced at high temperature under aggressive environmental conditions and applied in many branches of modern engineering materials due to its high melting point, high thermal and electrical conductivity, high thermal shock resistance, good oxidation resistance particularly at high temperature and excellent acid resistance including aqua regia. It has also been recognized to be a promising material for use as refractory neutron reflectors in gas-cooled fast neutron reactor cores (where temperature could reach to 2000 °C under incidental conditions) according to simulations based on the elastic scattering cross sections.[1-3] However, the Zr-Si intermetallics are not commercially available except $ZrSi_2$.

Actually, several conventional methods have been adopted for preparing Zr-Si intermetallics, such as mechanochemical synthesis,[4] self-propagating high-temperature synthesis (SHS),[5] reaction sintering,[3] Arc melting[6] and silicothermic reduction in vacuum at high temperature.[1] However, the expensive pure Zr and Si are typically used as raw materials in most of these methods, and they are the multi-step, high-cost and energy-extensive consumption processes. Furthermore, most of the products obtained by the above conventional methods are a mixture of silicides rather than a pure silicide. Therefore, a new method which can produce Zr-Si intermetallics with a designed composition through a simple and cost-effective way at moderate temperature is highly desired. Recently, the electrochemical deoxidation process, as a method for direct extraction of metals, semimetals or alloys by removing oxygen from solid oxides in molten alkali halides, has stimulated much interests. Previously, researchers have investigated the preparation of alloys or intermetallic compounds by electro-deoxidation of the mixed or complex oxides of the metals in molten salts, such as TiZr,[7] ZrCr,[8] TiMo,[9] NbTi,[10] $LaNi_5$,[11] Nb_3Sn,[12] TiW,[13] $TbNi_5$[14] and $TbFe_2$.[15] However, there have been few studies on the electrochemical preparation of Zr-Si intermetallics. Instead of preparation of the pure Zr and Si separately, Zr-Si intermetallics may be produced by direct electrochemical reduction of low-cost raw materials, such as nature ores or oxides, in one step.

In this study, the electrochemical deoxidation process was carried out for preparation of Zr-Si intermetallics from $ZrSiO_4$ and $ZrSiO_4$-SiO_2 mixed powders in molten $CaCl_2$-NaCl. In addition, the effects of the molar ratio of $ZrSiO_4$ to SiO_2 on the final product compositions and the electro-reduction pathways from $ZrSiO_4$ and SiO_2 to Zr-Si intermetallics were also investigated. The objective was to prepare Zr-Si intermetallics in a simple, cost-effective and environment friendly process.

Experimental

Commercial $ZrSiO_4$ (ZrO_2, 66%; Alfa Aesar) and AR grade of SiO_2 powders were used as raw materials. For $ZrSiO_4$-SiO_2 mixed samples, the mixture powders of $ZrSiO_4$ and SiO_2 with molar ratio of 1: 0.5 or 1:1 were firstly ball-milled with anhydrous alcohol for 4 h. Then, the $ZrSiO_4$ or $ZrSiO_4$-SiO_2 mixed powders were uniaxially pressed into cylindrical pellets (Ø 15×2 mm, 0.8 g) under a pressure of 6 MPa, which were finally sintered in air at 900 °C for 3 h. A schematic setup of the electrolysis cell is shown in Fig. 1. The sintered pellet was connected to a nickel wire through the hole drilled in its center (cathode). A graphite rod (Ø10×60 mm) was connected to a Kanthal wire (anode). The electrolyte of $CaCl_2$-NaCl eutectic

[a] School of Materials Science and Metallurgy, Northeastern University, Shenyang 110004, PR China.
[b] School of Materials Science and Engineering, Inner Mongolia University of Technology, Hohhot 010051, PR China.
[c] State Key Laboratory of Advanced Special Steel, Shanghai University, Shanghai 200072, PR China. E-mail: qianxu201@mail.neu.edu.cn
[d] Laboratory for Corrosion and Protection, Institute of Metal Research, Chinese Academy of Science, Shenyang 110016, PR China.

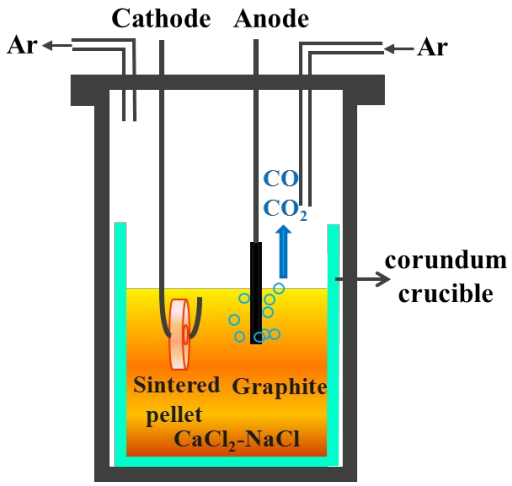

Fig. 1 Schematic diagram of the electrolysis cell in a stainless steel reactor.

mixture was firstly dried in a muffle furnace in air at 300 °C for 24 h and then put into a stainless steel reactor heated at 300 °C for 24 h in Ar atmosphere. Prior to the electrolysis, the $CaCl_2$-NaCl melt was pre-electrolyzed at 2.5 V for 2 h in order to remove electrochemically active impurities and moisture in the melt. The electrochemical reduction of $ZrSiO_4$ or $ZrSiO_4$-SiO_2 mixture was performed at a constant potential of 3.1 V and 800 °C. The incompletely and completely reduced specimens were obtained by terminating the electrochemical reduction after different reaction times ranging from 0.5 to 15 h.

After electrolysis, the pellet was lifted out of the melt and positioned at the top of the reactor to be cool down under the continuous flow of Ar. Then, the sample was washed with distilled water carefully to remove the adhering salts from the pellet and immersed in distilled water for 24 h, in ethanol for 12 h and finally dried in air at room temperature.

The phase composition of each sample was identified by X-ray diffraction (XRD, ultima IV, Rigaku, Japan). The microstructure and chemical composition of the samples were examined by scanning electron microscope and energy-dispersive X-ray spectroscopy (SEM and EDS, EVO18, Carl Zeiss, Germany).

Results and discussion

Zr-Si intermetallics with a designed composition were prepared by direct electrochemical reduction of $ZrSiO_4$ and SiO_2. The assembled cathode of the sintered $ZrSiO_4$ or $ZrSiO_4$-SiO_2 mixed pellet was electrolyzed with a graphite anode in molten $CaCl_2$-NaCl at 800 °C and under a constant voltage that is below the decomposition voltage of $CaCl_2$ (3.29 V).

Synthesis of Zr-Si intermetallics

The XRD patterns of the pellets with different molar ratios of $ZrSiO_4$ to SiO_2 sintered at 900 °C for 3 h are shown in Fig. 2. It reveals no peaks other than those of the starting materials, suggesting the absence of new compounds yielded in the sintering process.

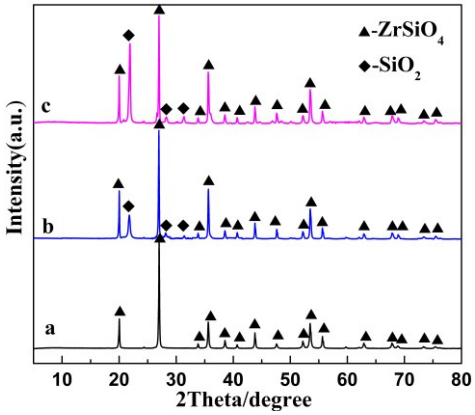

Fig. 2 XRD patterns of the pellets with different molar ratios of $ZrSiO_4$ to SiO_2 sintered at 900 °C for 3 h (a) $ZrSiO_4$; (b) $ZrSiO_4$:SiO_2 =1:0.5; (c) $ZrSiO_4$:SiO_2 =1:1.

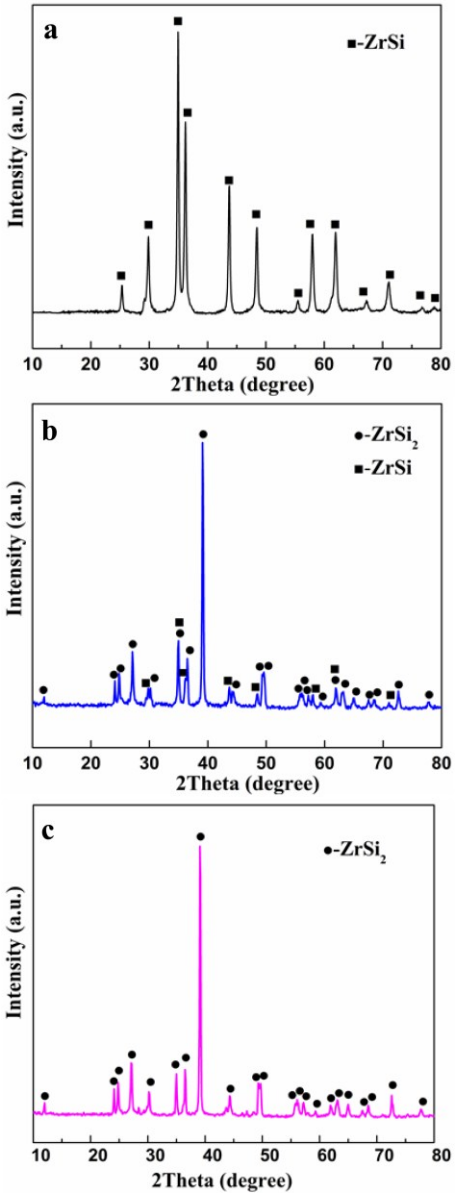

Fig. 3 XRD patterns of the products from electrolysis of the sintered pellets of (a) $ZrSiO_4$; (b) $ZrSiO_4$:SiO_2 =1:0.5; (c) $ZrSiO_4$:SiO_2=1:1 under 3.1 V at 800 °C for 15 h.

Fig. 3 shows the XRD patterns of the products from electrolysis of the sintered pellets with different molar ratios of $ZrSiO_4$ to SiO_2 at 3.1 V and 800 °C for 15 h. As shown in Fig. 3a, a single-phase ZrSi was obtained directly from $ZrSiO_4$. However, ZrSi and $ZrSi_2$ were found coexisting in the final product as $ZrSiO_4$:SiO_2 molar ratio equals to 1:0.5, shown in Fig. 3b. This may be due to the fact that the initial molar ratio of Si to Zr in this sample is 1.5:1. Furthermore, when the $ZrSiO_4$:SiO_2 molar ratio is 1:1, the final product was a single-phase $ZrSi_2$, as shown in Fig. 3c. All of these indicated that the $ZrSiO_4$ or $ZrSiO_4$-SiO_2 mixed pellet can be completely electro-reduced to Zr-Si intermetallics after 15 h. It also indicated that the phase composition of the final product can be controlled by adjusting the molar ratio of Si to Zr containing in the starting material.

The SEM images of the pellets completely electrolyzed (electrolyzed for 15 h) are shown in Fig. 4. The products of the electrolysis exhibit the nodular particles with grain size in the range of several hundred nanometers. The microstructure of the products obtained at different molar ratios of $ZrSiO_4$ to SiO_2 has a slight difference. According to the XRD analyses shown in Fig. 3a and 3c, $ZrSiO_4$ and $ZrSiO_4$-SiO_2 ($ZrSiO_4$:SiO_2=1:1) samples were completely electrolyzed to a single-phase ZrSi and $ZrSi_2$, respectively. Therefore, the SEM shows the particles have a similar morphology. However, the microstructure of the electrolysis product obtained from the $ZrSiO_4$-SiO_2 ($ZrSiO_4$:SiO_2=1:0.5) sample has different particle sizes, as shown in Fig. 4b. This may be due to the two kinds of silicide phases, ZrSi and $ZrSi_2$, coexisting in the products, as shown in Fig. 3b.

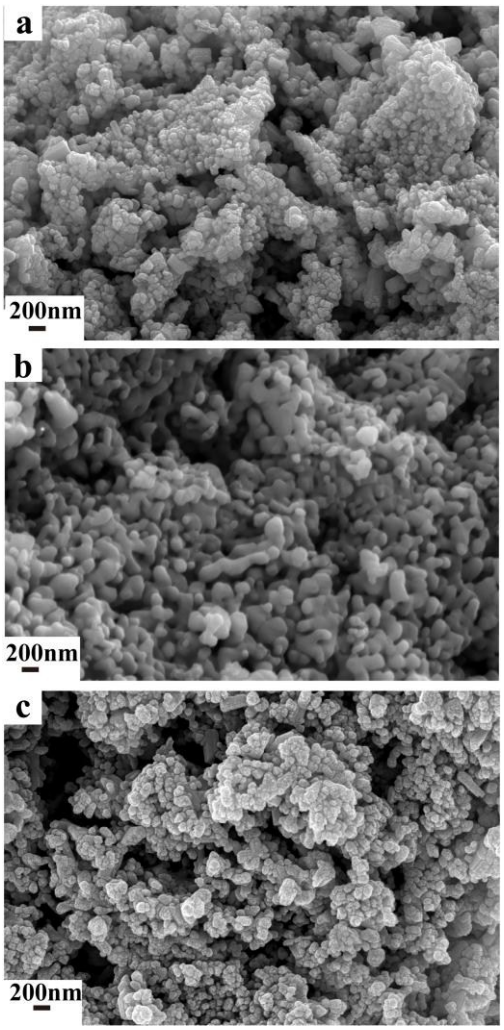

Fig. 4 SEM images of products from electrolysis of the sintered pellets of (a) $ZrSiO_4$; (b) $ZrSiO_4$:SiO_2 =1:0.5; (c) $ZrSiO_4$:SiO_2=1:1 under 3.1 V at 800 °C for 15 h.

Electro-reduction pathways

The typical current-time curves of the constant voltage electrolysis in molten $CaCl_2$-NaCl are presented in Fig. 5. It can be seen that all of the curves have similar shapes at the initial stage of the electrochemical reduction process (see the insert). The plot commences with a current peak and then the current declines gradually, through a few plateaus in the next 3 h, to a relatively small value. Thereafter the current remains relatively small and changes little with prolonging the time. This feature agrees with the reduction occurring at the metal/oxide/electrolyte three-phase interlines (3PIs).[16, 17] From the initial metal-oxide contacts, the 3PIs expand along the surface of the pellet first, leading to the current peak on the current-time plot. With the 3PIs propagate into the pellet along the depth direction, the current declines to a relatively constant value. The current plateaus are likely to indicate that the reduction goes through multiple steps.

To identify the reaction pathways of the electrochemical reduction, a series of electrolysis experiments of $ZrSiO_4$-SiO_2 ($ZrSiO_4$:SiO_2=1:0.5) mixed pellets were carried out with different electrolysis durations ranging from 0.5 to 12 h.

Fig. 6a and 6b show the XRD patterns of partially reduced samples for 0.5 h and 1 h, respectively. The results show that the samples after electrolysis for 0.5 h and 1 h are primarily composed of unreacted $ZrSiO_4$ and SiO_2. Besides the typical XRD peaks related to the predominant phases of $ZrSiO_4$ and

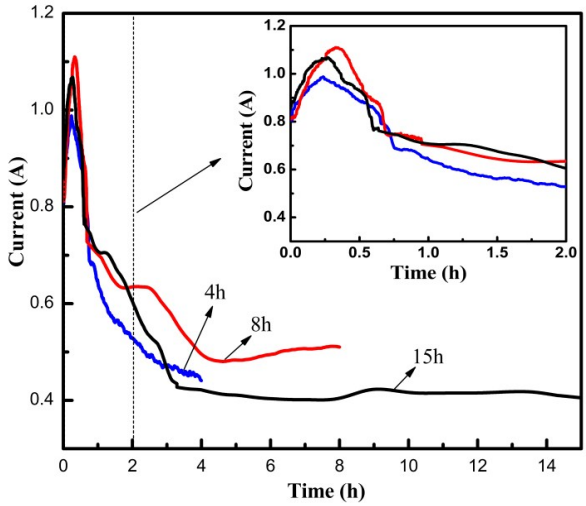

Fig. 5 Typical current-time plots recorded during constant voltage electrolysis of the sintered $ZrSiO_4$-SiO_2 ($ZrSiO_4$:SiO_2 =1:0.5) mixed pellets at 3.1 V and 800 °C for different times in $CaCl_2$-NaCl melt, the insert shows the enlarged drawing of the initial part of the current-time plots.

Journal Name

ARTICLE

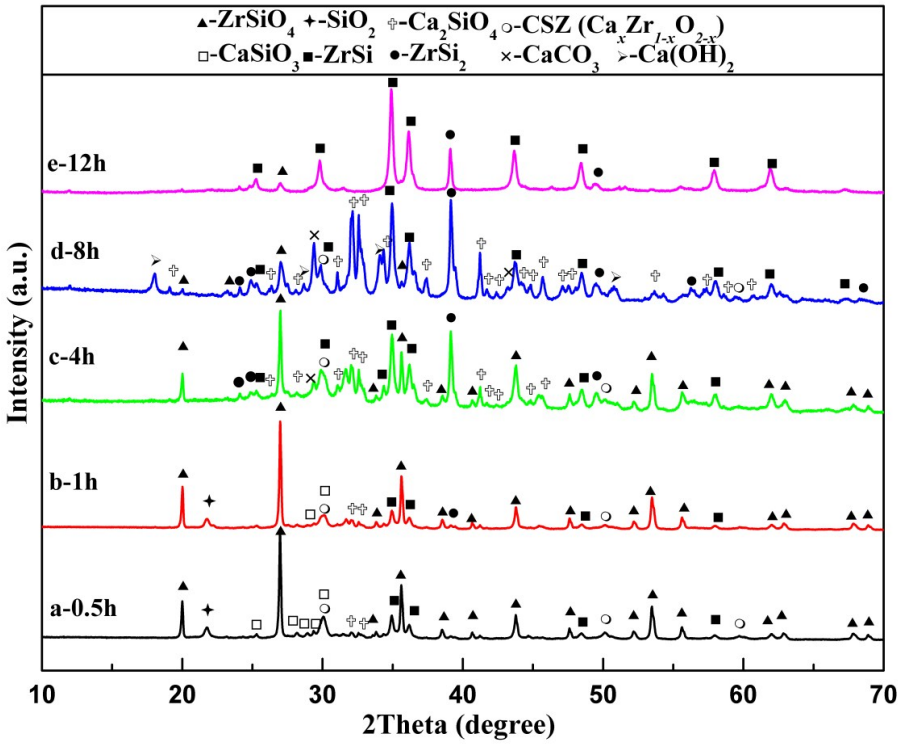

Fig. 6 XRD patterns of the $ZrSiO_4$-SiO_2 ($ZrSiO_4$:SiO_2 =1:0.5) mixed pellets electrolyzed at 3.1 V and 800 °C in $CaCl_2$-NaCl melt for (a) 0.5 h; (b) 1 h; (c) 4 h; (d) 8 h; (e) 12 h.

Table 1 Standard Gibbs free-energy change and reaction potential of different reactions at 800 °C

Reaction	ΔG^{Θ}(kJ·mol^{-1})	Theoretical Reaction Potential (V)
$Ca_2SiO_{4(s)} + C_{(s)} = Si_{(s)} + 2CaO_{(s)} + CO_{2(g)}$ (8)	455.691	-1.18
$Ca_xZr_{1-x}O_{2-x\,(s)} + (1-x)C_{(s)} = (1-x)Zr_{(s)} + xCaO_{(s)} + (1-x)CO_{2(g)}$ (9)	≈387.101	≈-1.18
$CaSiO_{3(s)} + C_{(s)} = Si_{(s)} + CaO_{(s)} + CO_{2(g)}$ (10)	412.496	-1.07

SiO_2, the peaks with small intensities are related to calcia-stabilized zirconia (CSZ) and calcium silicates ($CaSiO_3$ and Ca_2SiO_4), whereas the remaining XRD peaks are ascribed to the ZrSi and $ZrSi_2$ phases. CSZ ($Ca_xZr_{1-x}O_{2-x}$) and calcium silicates ($CaSiO_3$ and Ca_2SiO_4) phases are detected, indicating that $ZrSiO_4$ was decomposed into calcium-containing intermediate compounds (CSZ, $CaSiO_3$ and Ca_2SiO_4) by combination with calcium oxide (CaO) which is formed during the drying of the melt [18-20] or by the electrochemically generated O^{2-} ions and Ca^{2+} ions from the melt, and the corresponding reactions are shown in Eqs. (1) and (2). In addition, SiO_2 containing in the starting material also reacted with CaO to form $CaSiO_3$ or Ca_2SiO_4. $ZrSiO_4$ or SiO_2 is a typical insulator,[21] whereas CSZ is a good ionic conductor and calcium silicate is a poor conductor.[22] The incorporation of CaO into $ZrSiO_4$ or SiO_2 transforms an insulated cathode into a good ionic and poor electronic conductor, which is beneficial to the transfer of the produced O^{2-}. Meanwhile, electro-deoxidation of the cathode pellet has occurred, which can be confirmed by the appearance of ZrSi and $ZrSi_2$ phases. This may imply that $CaSiO_3$ and Ca_2SiO_4 were reduced into Si by Eqs. (3) and (4) respectively, and CSZ ($Ca_xZr_{1-x}O_{2-x}$) was reduced into Zr by Eq. (5). Almost immediately, the follow-on reactions between Zr and Si occurred to form ZrSi and $ZrSi_2$ intermetallic compounds by Eqs. (6) and (7) shown as following.

$$(1-x)ZrSiO_4 + Ca^{2+} + O^{2-} = Ca_xZr_{1-x}O_{2-x} + (1-x)CaSiO_3 \quad (1)$$
$$(1-x)ZrSiO_4 + (2-x)Ca^{2+} + (2-x)O^{2-} = Ca_xZr_{1-x}O_{2-x} + (1-x)Ca_2SiO_4 \quad (2)$$
$$CaSiO_3 + 4e = Si + CaO + 2O^{2-} \quad (3)$$
$$Ca_2SiO_4 + 4e = Si + 2CaO + 2O^{2-} \quad (4)$$
$$Ca_xZr_{1-x}O_{2-x} + 4(1-x)e = (1-x)Zr + xCaO + 2(1-x)O^{2-} \quad (5)$$

$Zr + Si = ZrSi$ (6)

$Zr + 2Si = ZrSi_2$ (7)

It is notable that no elemental Si and Zr phases are observed, which may imply that calcium silicates ($CaSiO_3$, Ca_2SiO_4) and CSZ ($Ca_xZr_{1-x}O_{2-x}$) phases simultaneously reduced to Si and Zr by ionizing oxygen, subsequently forming ZrSi and $ZrSi_2$.The theoretical potentials for the overall reactions which take place in the electro-deoxidation cell with the graphite anode are calculated using thermodynamic data[22, 23] and shown in Table 1. The standard states for gases and solids are the gases at standard pressure (10^5 Pa) and the pure substances, respectively. It should be noted that the standard Gibbs free-energy change or the potential calculated for Eq. (9) is an approximate value, because the thermodynamic data of $Ca_{0.17}Zr_{0.83}O_{1.83}$ was used to approximately replace that of $Ca_xZr_{1-x}O_{2-x}$. It can be seen that the potentials required for reduction of Ca_2SiO_4 and $Ca_xZr_{1-x}O_{2-x}$ are almost equal. While

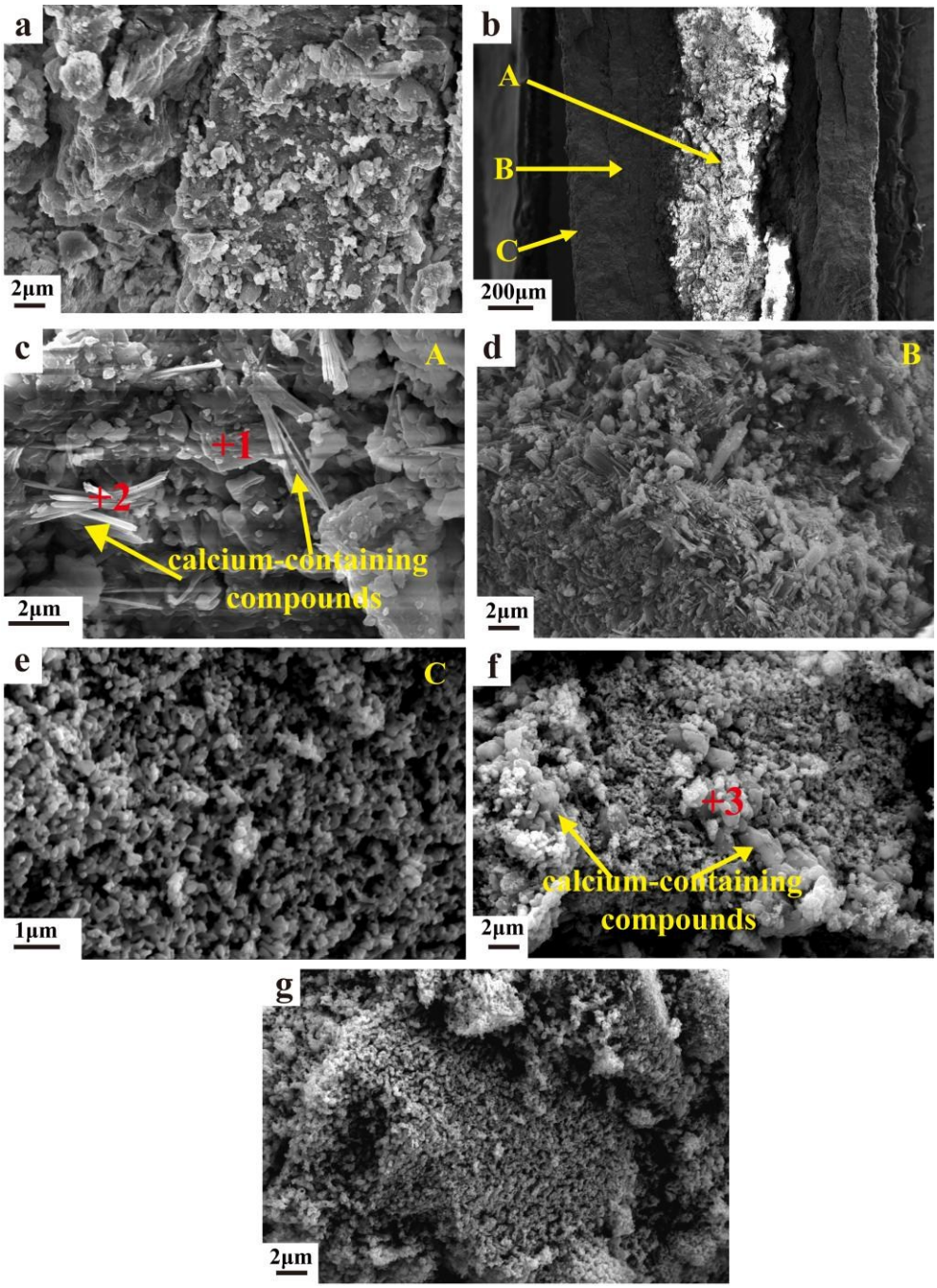

Fig. 7 SEM images of (a) the pellet of the $ZrSiO_4$-SiO_2 ($ZrSiO_4$:SiO_2 =1:0.5) mixed powders prepared by pressing at 6 MPa and sintering at 900 °C for 3 h. (b) the cross-section of the $ZrSiO_4$-SiO_2 ($ZrSiO_4$:SiO_2 =1:0.5) mixed pellet electrolyzed at 3.1 V and 800 °C in $CaCl_2$-NaCl melt for 1 h; (c) the core of the inner layer of the sample shown in panel b; (d) the core of the outer layer of the sample shown in panel b; (e) the surface layer of the sample shown in panel b at a higher magnification; (f) the $ZrSiO_4$-SiO_2 ($ZrSiO_4$:SiO_2 =1:0.5) mixed pellets electrolyzed for 8 h; (g) the $ZrSiO_4$-SiO_2 ($ZrSiO_4$:SiO_2 =1:0.5) mixed pellets electrolyzed for 12 h.

Journal Name

ARTICLE

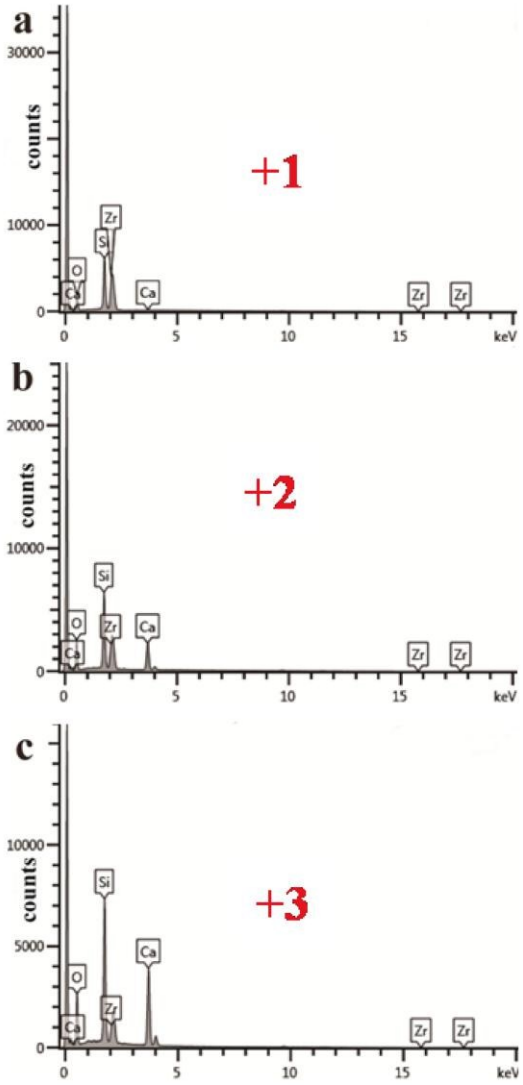

Fig. 8 EDX spectrum obtained from (a) point analysis 1 marked in Fig. 7c; (b) point analysis 2 marked in Fig. 7c; (c) point analysis 3 marked in Fig. 7f.

the potential required for reduction of $CaSiO_3$ is a little lower than that of Ca_2SiO_4 and $Ca_xZr_{1-x}O_{2-x}$, so the reaction (3), (4) and (5) may proceed simultaneously.

Fig. 7b shows the SEM image of the cross-section of the partially reduced sample for 1 h, showing the typical "sandwich" structure, which can be observed visually as a white ceramic inner layer surrounded by the dark grey outer layer. The inner layer of the sample, as shown in Fig. 7c, is similar to the precursor sample after sintering (Fig. 7a), indicating that the inner layer remains largely unreacted after 1 h reduction. In combination of the XRD (Fig. 6b) and EDS (Fig. 8a) results, it may consist of $ZrSiO_4$ and SiO_2. Whereas, a few fiber-like particles emerge from the initial coarse and monolithic particles, which is identified by XRD (Fig. 6b) and EDS (Fig. 8b) to be the transformation of $ZrSiO_4$ and SiO_2 to calcium-containing intermediate compounds ($CaSiO_3$, Ca_2SiO_4 and CSZ). Fig. 7d shows the morphology of the middle of the outer layer of the sample electrolyzed after 1 h. It can be seen that the fiber-like particles grow gradually and fill the space in more than one dimension, indicating that more calcium-containing intermediate compounds were formed than that in the inner layer of the pellet. The surface layer of the pellet in Fig. 7b at higher magnification is demonstrated in Fig. 7e, which looks like metallic phases and is composed of interconnected nodular particles. The nodules should be ZrSi and $ZrSi_2$ according to the XRD analyses (Fig. 6b). As depicted, the electro-reduction of the cathode pellet proceeds inward from the pellet's surface.

Fig. 6c and 6d show the XRD patterns of partially reduced samples for 4 h and 8 h, respectively. With the electrolysis time prolonging to 8 h, it can be seen that the intensities of the peaks ascribed to $ZrSiO_4$ decreased significantly, simultaneously with the rise of the peaks ascribed to the calcium-containing intermediate compounds (Ca_2SiO_4, CSZ) and metallic phases (ZrSi, $ZrSi_2$). $CaCO_3$ was most likely formed by the secondary reaction between CaO and CO_2 which was generated on the graphite anode and dissolved in the melt during the reduction. It is noteworthy that the minor phase of $Ca(OH)_2$ was detected after 8h electrolysis. It was thought to originate from the electrolytes during the water cleaning treatment of the cathodic product ($Ca+2H_2O=Ca(OH)_2+H_{2(g)}$),[24] which indicates that the decomposing of CaO occurred and a very small quantities of reduced calcium dissolved in the melts. Therefore, the chemical reduction may assist the reduction process and should become non-negligible during the later stages of the process.

Fig. 7f shows the SEM image of the partially reduced sample after 8 h reduction and two types of particles are observed. According to the XRD (Fig. 6d) and EDS (Fig. 8c) analyses, the dense aggregates of irregularly large particles with an average size less than 2 μm mainly consist of calcium-containing intermediate compounds (Ca_2SiO_4, CSZ), whereas the relatively fine nodular particles should be composed of metallic phases.

Fig. 6e and Fig. 7g show the XRD pattern and SEM image of the partially reduced sample after 12 h electrolysis, respectively. The results show that the sample primarily consists of ZrSi and $ZrSi_2$ phases with fine and homogeneous particles. The gradual reduction of the pellet and the

Journal Name

ARTICLE

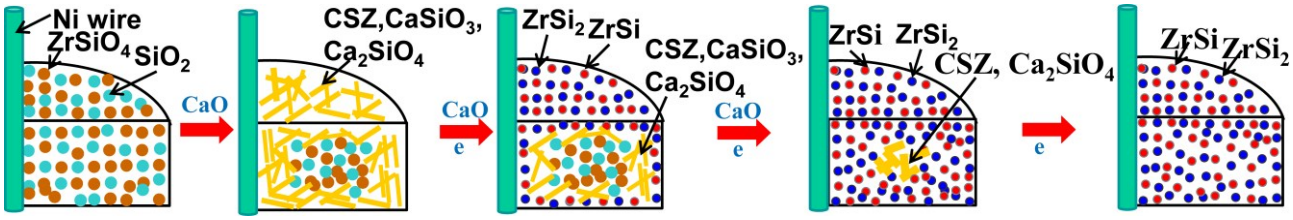

Fig. 9 Schematic illustration of the direct electrolytic reduction of the solid $ZrSiO_4$-SiO_2 mixture to Zr-Si intermetallics in $CaCl_2$-NaCl melt.

successive formation of metallic phases produce the finer and more uniform microstructure. However, the relatively high and constant current (around 0.4 A) was still observed, as shown in Fig. 5. It may be due to the compensating effects of the slowly declining oxide ion current, originating from the removal of oxygen of the cathode, and the slowly rising electronic background current, generating from the dissolved calcium species and the free carbon which was observed on the surface of the molten salt after the experiment. [25]

According to the above discussion, the reduction mechanism of the $ZrSiO_4$-SiO_2 cathode by the electrochemical deoxidation process is schematically proposed in Fig. 9. Firstly, by the reaction of CaO with $ZrSiO_4$ or SiO_2, the calcium silicates ($CaSiO_3$, Ca_2SiO_4) and CSZ ($Ca_xZr_{1-x}O_{2-x}$) intermediate phases were formed in the cathode and located at the same place. Secondly, the calcium silicates ($CaSiO_3$, Ca_2SiO_4) and CSZ ($Ca_xZr_{1-x}O_{2-x}$) were simultaneously reduced into Si and Zr respectively, which were combined to form ZrSi and $ZrSi_2$ immediately. Finally, with the further formation and successive reduction of calcium-containing intermediate phases inwardly, the $ZrSiO_4$-SiO_2 mixed cathode was completely reduced to Zr-Si intermetallics with a fine and uniform microstructure. It is worth mentioning that the presence of the dissolved calcium may interfere with the electrochemical reduction pathway during the later stages of the process.

Conclusions

Zr-Si intermetallic compounds were controllably prepared from $ZrSiO_4$ or $ZrSiO_4$-SiO_2 mixed precursors by the electrochemical deoxidation process in eutectic $CaCl_2$-NaCl molten salt. It was found that the final product keeps the molar ratio of Si to Zr in the staring materials. For pure $ZrSiO_4$, a single phase ZrSi was obtained. A mixture of ZrSi and $ZrSi_2$ was found coexisting in the final product of $ZrSiO_4$-SiO_2 ($ZrSiO_4$:SiO_2 =1:0.5) mixture. A single-phase $ZrSi_2$ was formed as $ZrSiO_4$:SiO_2 molar ratio is 1:1. All of the products were composed of nodular particles with particle size in the range of several hundred nanometers.

The reduction mechanism of the $ZrSiO_4$-SiO_2 cathode is summarized as following. Firstly, the solid $ZrSiO_4$ or SiO_2 interacts with CaO to form calcium silicates ($CaSiO_3$, Ca_2SiO_4) and CSZ ($Ca_xZr_{1-x}O_{2-x}$) phases. Then, calcium silicates ($CaSiO_3$, Ca_2SiO_4) and CSZ ($Ca_xZr_{1-x}O_{2-x}$) are electro-deoxidized to Si and Zr. The follow-on reaction occurs between Zr and Si to form Zr-Si intermetallics.

Acknowledgements

The authors acknowledge the financial support of the National Natural Science Foundation of China (Grant No. 51174055).

References

1. A. Tkachenko and T. Y. Kosolapova, *Soviet Powder Metallurgy and Metal Ceramics*, 1968, **7**, 178-181.
2. I.-J. Cho, K.-T. Park, S.-K. Lee, H. H. Nersisyan, Y.-S. Kim and J.-H. Lee, *Chem. Eng. J.*, 2010, **165**, 728-734.
3. J. Canel, J. Zaman, J. Bettembourg, M. Flem and S. Poissonnet, *Int. J. Appl. Ceram. Technol.*, 2006, **3(1)**, 23-31.
4. B. K. Yen, *J. Alloys Compd.*, 1998, **268**, 266-269.
5. N. Bertolino, U. Anselmi-Tamburini, F. Maglia, G. Spinolo and Z. Munir, *J. Alloys Compd.*, 1999, **288**, 238-248.
6. N. Salpadoru and H. Flower, *Metall. Mater. Trans. A*, 1995, **26A**, 243-257.
7. J. Peng, H. L. Chen, X. B. Jin, T. Wang, D. H. Wang and G. Z. Chen, *Chem. Mater.*, 2009, **21**, 5187-5195.
8. J. Peng, Y. Zhu, D. H. Wang, X. B. Jin and G. Z. Chen, *J. Mater. Chem.*, 2009, **19**, 2803-2809.
9. R. Bhagat, M. Jackson, D. Inman and R. Dashwood, *J. Electrochem. Soc.*, 2008, **155(6)**, E63-E69.
10. X. Y. Yan and D. J. Fray, *Adv. Funct. Mater.*, 2005, **15**, 1757-1761.
11. Y. Zhu, D. H. Wang, M. Ma, X. H. Hu, X. B. Jin and G. Z. Chen, *Chem. Commun.*, 2007, 2515-2517.
12. B. A. Glowacki, D. J. Fray, X. Y. Yan and G. Chen, *Physica C*, 2003, **387**, 242-246.

13. K. Dring, R. Bhagat, M. Jackson, R. Dashwood and D. Inman, *J. Alloys Compd.*, 2006, **419**, 103-109.
14. G. H. Qiu, D. H. Wang, X. B. Jin and G. Z. Chen, *Electrochim. Acta*, 2006, **51**, 5785-5793.
15. G. H. Qiu, D. H. Wang, M. Ma, X. B. Jin and G. Z. Chen, *J. Electroanal. Chem.*, 2006, **589**, 139-147.
16. Y. Deng, D. H. Wang, W. Xiao, X. B. Jin, X. H. Hu and G. Z. Chen, *J. Phys. Chem. B,* 2005, **109**, 14043-14051.
17. W. Xiao, X. B. Jin, Y. Deng, D. H. Wang, X. H. Hu and G. Z. Chen, *ChemPhysChem*, 2006, **7**, 1750-1758.
18. G. Z. Chen and D. J. Fray, *J. Electrochem. Soc.*, 2002, **149**, E455-E467.
19. C. Schwandt and D. Fray, *Electrochim. Acta*, 2005, **51**, 66-76.
20. K. Hirota, T. Okabe, F. Saito, Y. Waseda and K. Jacob, *J. Alloys Compd.*, 1999, **282**, 101-108.
21. R. Terki, G. Bertrand and H. Aourag, *Microelectron. Eng.*, 2005, **81**, 514-523.
22. K. S. Mohandas and D. J. Fray, *Metall. Mater. Trans. B*, 2009, **40**, 685-699.
23. A. Roine, HSC Chemistry, version 6.0, Outokumpu Research Oy, Pori, Finland, 2006
24. X. Y. Yan, M. I. Pownceby, M. A. Cooksey and M. R. Lanyon, *Mineral Processing and Extractive Metallurgy*, 2009, **118**, 23-34.
25. C. Schwandt and D. J. Fray, *Z. Naturforsch., A: Phys. Sci.*, 2007, **62**, 655-670.

Graphical Abstract

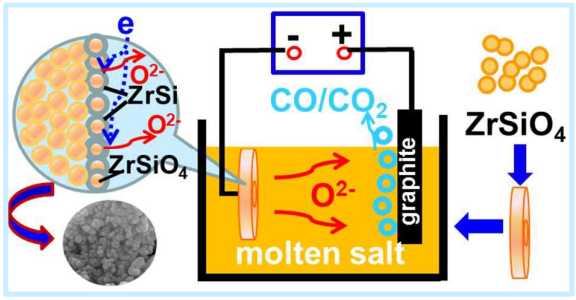

Zr-Si intermetallics with a designed composition were prepared by direct electrochemical reduction of $ZrSiO_4$ and SiO_2 in one step.